Presented at the Research Congress 2013
De La Salle University Manila
March 7-9, 2013

DIRECT AND INDIRECT EVAPORATIVE COOLING USING CERAMIC ABSORBERS

Mar John V. Macabodbod , John Matthew S. Macalalad, Joseph P. Talampas,
John Brian C. Tan, and Martin Ernesto L. Kalaw
Mechanical Engineering Department, De La Salle University
Manila, Philippines

Abstract: The use of HVAC/R systems is projected to continue to take a major part of world energy consumption. However, its increasing application, together with decreasing energy resources, ozone depletion and climate change bring the need for greener HVAC/R technologies. One such technology that is already commercially available is evaporative cooling. It is seen that there is a need to understand the limitations of evaporative cooling as a HVAC/R alternative in the Philippines.

An experimental set-up demonstrating direct and indirect evaporative cooling was designed, fabricated and tested. The humidity, water temperature, water distribution, and air velocity were the control variables. The results show the following: 1) Air flow rate is directly proportional to air temperature drop through the direct and indirect evaporative cooling stages, 2) Water flow rate is directly proportional to direct and indirect evaporative cooling efficiency and COP, 3) Humidity is inversely proportional to latent heat absorption, and 4) Water temperature drop to the sump is inversely proportional to direct evaporative cooling efficiency.

On a per session basis, the set-up was able to achieve temperature drops of as much as 2.1°C for supply air at the heat exchanger, 1.6°C for supply air through the direct evaporative cooling coil, 3.7°C for water droplets from the top reservoir to the sump, a COP of 4.8, and direct evaporative cooling efficiency of 92.373%.

Key Words: evaporative cooling; ceramic absorbers; HVAC/R

1. INTRODUCTION

Direct evaporative cooling is achieved through the interaction of higher temperature, lower humidity air and liquid water. The high latent heat of evaporation of water is taken from the high temperature air resulting in lower temperature but higher humidity air. Indirect evaporative cooling on the other hand uses the same concept of cooling but without the intent of placing the cooled subject in contact with water. A conductive wall separates the evaporative cooling process from the cooled subject.

Porous ceramics were used as an evaporative media because of their good thermal conductivity and porosity. Studies discovered that ceramic porosity have a major effect on evaporation (ICT International, 2009; He, J., Hoyano, A., 2010; Shao, L. et al, 2003; Riffat, S., Zhu, J. 2003; Velasco Gomez et al, 2005).

Studies have been done in determining the viability of evaporative coolers in various climates. Evaporative coolers perform best in hot and arid conditions. There are studies however on the use of evaporative coolers in humid conditions such as were done in Nigeria, India, Hong Kong, Spain and Israel (Anyanwu, E. 2004; Jain, D. 2006; Jain, S et al 1995; Fong, K et al 2010; Rey Martínez et al 2010; Navon, R., Arkin, H. 1994).

2. METHODOLOGY

The setup is divided into two parts: the copper-ceramic coil side and the heat exchanger side. The schematic of the flow is shown in Figure 1 below:

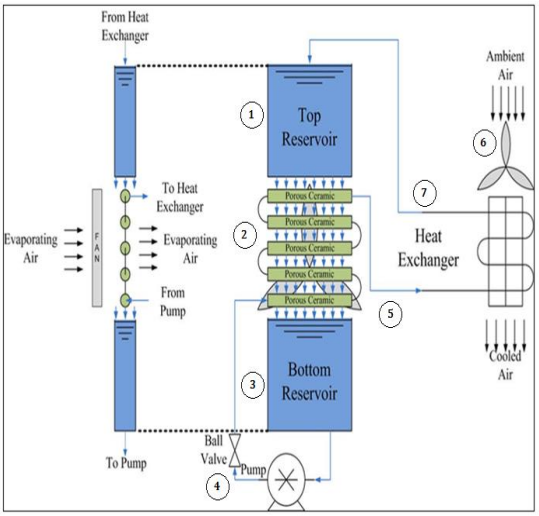

Figure 1. Direct-Indirect Evaporative cooler schematic

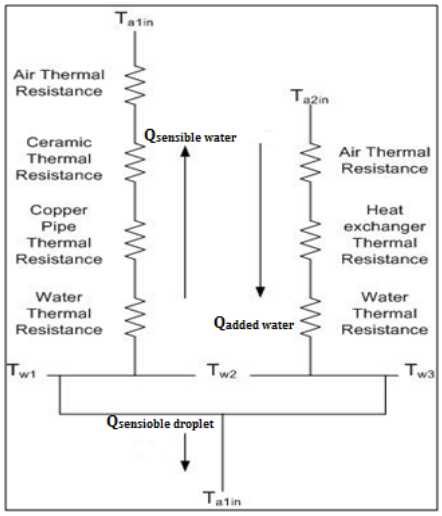

Figure 2.Thermal resistance model.

The operation of the system is summarized below:

1. Water starts at the top reservoir (used as the starting reference point).
2. The system is turned on. Water from the top reservoir drips through the holed plates and wets the ceramic.
3. Direct evaporative cooling. A fan evaporates some of the water in the ceramic, removing heat from the copper-ceramic coil. Un-evaporated water, which also experiences cooling, drips to the sump.
4. Un-evaporated water and water at the sump is pumped through the copper-ceramic coil. As it flows inside the copper-ceramic coil, it is cooled further due to the effect of evaporative cooling on the ceramic and copper piping in which it is enclosed.
5. Cooled water exits the copper-ceramic coil and enters the heat exchanger.
6. Indirect evaporative cooling. A fan blows outside air through the heat exchanger. Water flowing through the heat exchanger, absorbs heat and thereby sensibly cools the air.
7. Water exits the heat exchanger at a higher temperature and goes back to the top reservoir to repeat the cycle.

Equation [1] shows the mass transfer for water that drops to the ceramic (between evaporated and un-evaporated water). The heat transfer Equation [2] shows the sensible and latent heat transfer for air and water. It measures the overall effect of the cooling tower effect and the indirect evaporative cooling induced by the porous ceramic. Equations [3] represent the heat transfer in the heat exchanger.

$$m_{a1_{out}} = m_{a1_{in}} + m_{a1_{in}}\left[1 + \left(H_{1_{out}} - H_{a1_{in}}\right)\right] \quad \text{(eq. 1)}$$

$$Q_1 = m_{a1_{in}}\left[c_{p_{air}}\left(T_{a1_{out}} - T_{a1_{in}}\right) + \left(H_{a1_{out}} - H_{a1_{in}}\right)h_d\right] = m_w c_{water}(T_{w1} - T_{w2}) + m_w c_{water}(T_{w2} - T_{w3}) \quad \text{(eq. 2)}$$

$$Q_2 = m_w c_{water}(T_{w3} - T_{w2}) = m_{a2_{in}} c_{p_{air}}(T_{a2_{in}} - T_{a2_{out}}) \quad \text{(eq. 3)}$$

where:

$m_{a1_{in}}, m_{a1_{out}}$ = entering and exiting mass flow rate of evaporating air, kg/s

$m_{a2_{in}}$ = entering mass flow rate of cooling air, kg/s

$H_{a1_{in}}, H_{a1_{out}}$ = entering and exiting humidity ratio of evaporating air, kgv/kgda

Q_1 = total heat rejected due to cooling tower effect, kW

m_w = mass flow rate of cooled water, kg/s

T_{w1}, T_{w2}, T_{w3} = water temperature entering the copper - ceramic coil, entering the heat exchanger and leaving the heat exchanger, ^oC

Q_2 = total heat absorbed by the water in the heat exchanger, kW

$T_{a2_{in}}, T_{a2_{out}}$ = entering and exiting temperature of cooling air, ^oC

The thermal resistance model of Riffat and Zhu (2003) was useful in creating the thermal resistance model of the set-up as shown in Figure 2. The thermal resistances are evaluated using eqs. 4 to 7.

$$R_{air,out} = \frac{1}{\pi h_o d_{p,o} L_p} \quad \text{(eq. 4)}$$

$$R_{pipe} = \frac{\ln(d_{p,o}/d_{p,i})}{2\pi k_p L_p} \quad \text{(eq. 5)}$$

$$R_{ceramic} = \frac{\ln(d_{c,o}/d_{c,i})}{2\pi k_c L_c} \quad \text{(eq. 6)}$$

$$R_{water,in} = \frac{1}{\pi h_i d_{p,i} L_p} \quad \text{(eq. 7)}$$

where:

$R_{air,out}$ = thermal resistance from outside air to outside pipe surface, $^oC/W$

R_{pipe} = thermal resistance across pipe layer, $^oC/W$

$R_{ceramic}$ = thermal resistance across ceramic layer, $^oC/W$

$R_{water,in}$ = thermal resistance from inside pipe surface to water, $^oC/W$

$d_{p,o}, d_{p,i}, L_p, k_p$ = outside and inside diameter, length, and thermal conductivity of the pipe, m

$d_{c,o}, d_{c,i}, L_c, k_c$ = outside and inside diameter, length, and thermal conductivity of the ceramic, m

h_o, h_i = convection coefficien t outside and inside, $W/m^{2\,o}C$

Actual conditions measured during experimentation were dry bulb temperature, relative humidity, and air flow rate. The dry bulb temperature was measured using LM35 temperature sensors. These sensors were calibrated using digital and mercury thermometers. Relative humidity was measured using HS1101 RH Capacitive Sensors. These sensors were calibrated using a digital hygrometer. Air flow rate was measured using a digital anemometer.

The temperature and relative humidity sensors were installed (twelve for temperature, two for humidity) at the inlets and exit points for air and water flow at different components of the set-up. From the measuring points, the sensors were wired to the Agilent 9490A Data Acquisition System for automatic data recording at frequent intervals (readings every five seconds). The results are exported to MS Excel files.

Experiments were made in varying fan speed/air flow rate at the copper-ceramic coil, water distribution/water flow rate, water temperature, and the presence of desiccant (activated carbon). Fan speeds were varied between high (9.0 m/s) and low (3.0 m/s), while the fan speed at the heat exchanger was kept constant (4.5 m/s). Water distribution was varied by changing the opening of the valve (at the discharge of the pump) between fully-open (0.259 L/s) and partially-open (0.060 L/s). The set-up is run on tap water, which changes temperature during different times of the day. Hence water temperature was varied by running the set-up with tap water in the morning (9:00am), noon (12:00pm) and afternoon (5:00pm). For the desiccant, half of the cases were tested with the desiccant, while the other half without the desiccant. It must be noted that the presence of the desiccant decreases the air flow rate of the heat exchanger; the high speed was reduced from 9.0 m/s to 2.617 m/s while the low speed was reduced from 3.0 m/s to 1.967 m/s. Table 1 shows the days and the cases in which the set-up was run.

Table1. Experimental Parameters Matrix

Day	Case	Desiccant	Fan Speed	Water Flow Rate
8	1	0	0	0
7	2	0	0	1
2	3	0	1	0
1	4	0	1	1
6	5	1	0	0
5	6	1	0	1
4	7	1	1	0
3	8	1	1	1

Legend: Desiccant (0 for w/o desiccant, 1 for w/ desiccant).Fan Speed (0 for low speed, 1 for high speed).Water flow rate (0 for partially-open valve, 1 for fully-open valve).

3. RESULTS AND DISCUSSION

Direct Evaporative cooling: Sump Water Temperature

To determine which parameter/s significantly affect/s direct evaporative cooling process of the system, the sump temperature (temperature change from the top reservoir) was used to represent direct evaporative cooling. It is seen from Figure 3 that the air flow rate behaves in parabolic manner such that its lowest temperature is achieved at 2.617 m/s. Lower than 2.617 m/s leads to an increase in sump water temperature. The lower flow rates lead to a saturation of air in the copper-ceramic coil, thereby limiting the evaporative cooling possible and limiting the temperature drop for the water droplets.

Indirect Evaporative Cooling: Air Temperature at Heat Exchanger

Indirect evaporative cooling is best exhibited by the exit air temperature at the heat exchanger. It is seen from Figure 4 that the behavior of the air temperature also follows a parabolic path vis a vis the fan speed with 2.617 m/s giving best results.

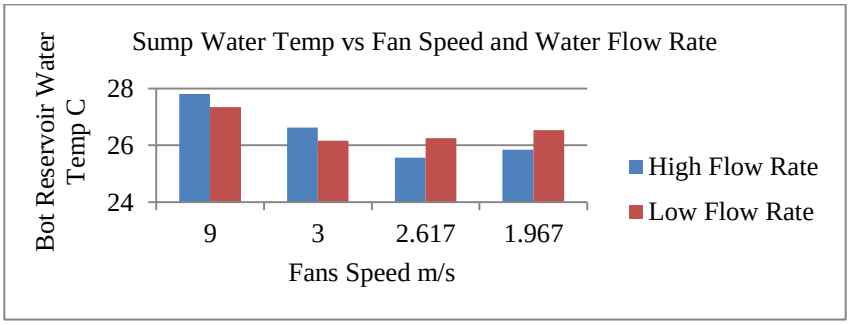

Figure 3. Correlation of sump water temperature as function of fan speed and water flow rate.

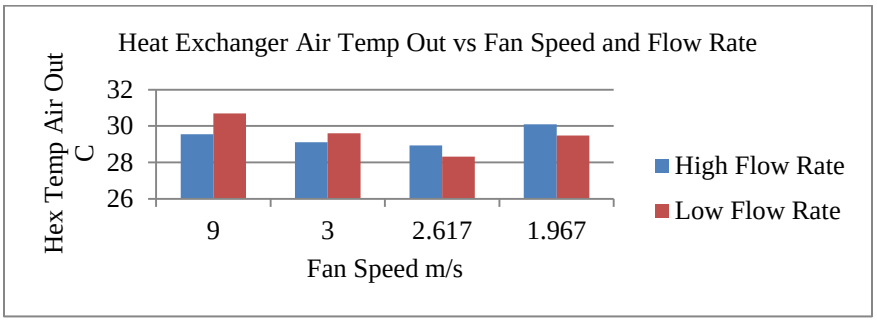

Figure 4. Correlation of heat exchanger air temperature outlet as a function of fan speed and water flow rate.

Coefficient of Performance

The overall performance of the cooling system was quantified through the COP. This performance factor was analyzed to better determine and predict the best operating conditions for the set-up. From Figure 5, the most stable COP for both water flow rate levels were observed at the 2.617 m/s setting.

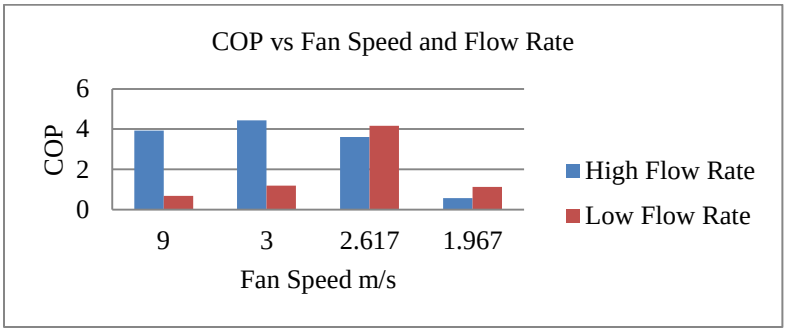

Figure 5.Correlation of COP as a function of fan speed and water flow rate.

4. CONCLUSIONS

The set-up demonstrated the following relations: 1) Air flow rate is directly proportional to air temperature drop through the direct and indirect evaporative cooling stages, 2) Water flow rate is directly proportional to direct and indirect evaporative cooling efficiency and COP, 3) Humidity is inversely proportional to latent heat absorption, and 4) Water temperature at the sump is inversely proportional to direct evaporative cooling efficiency.

On a per session basis, the set-up was able to achieve temperature drops of as much as 2.1°C for supply air at the heat exchanger, 1.6°C for supply air through the copper-ceramic coil, 3.7°C for water droplets from the top reservoir to the sump, a COP of 4.8, and direct evaporative cooling efficiency of 92.373%.

5. REFERENCES

Anyanwu, E. (2004). Design and measured performance of a porous evaporative. *Energy Conversion and Management 45* , 2187 - 2195.

Ao, C., Lee, S. (2005). Indoor air purification by photocatalyst TiO2 immobilized on activated carbon filter installed in an air cleaner. *Chemical Engineering Science 60*. 103-109

Fong, K., Chow, T., Lee, C., Lin, Z., & Chan, L. (2010). Advancement of solar desiccant cooling system for building use in subtropical Hong Kong. *Enegy and Buildings, XLII*, 2386-2399.

He, J., Hoyano, A. (2010). Experimental study of cooling effects of a passive evaporative cooling wall constructed of porous ceramics with high water soaking-up ability. *Building and Environment 45, 461-472*

ICT International. (2009). *Properties of Porous Ceramics*. Retrieved March 11, 2011, from ICT: http://www.ictinternational.com.au/ceramicsproperties.htm

Jain, D. (2006). Development and Testing of two-stage Evaporative Cooler. *Building and Environment 42*. 2549-2554

Jain, S., Dhar, P., & Kaushik, S. (1995). Evaluation of solid-desiccant-based evaporative cooling cycles for typical hot and humid climates. *International Journal of Refrigeration, XVIII* (5), 287-296.

Navon, R., Arkin, H. (1994). Feasibility of Direct-Indirect Evaporative Cooling for Residences, Based on Studies with a Desert Cooler. *Building and Environment* , 393-399.

Rey Martínez, F., Velasco Gómez, E., Tejero González, A., & Flores Murrieta, F. (2010). Comparative study between a ceramic evaporative cooler (CEC) and an air-source heat pump applied to a dwelling in Spain. *Energy and Buildings, XLII*, 1815-1822.

Riffat, S., Zhu, J. (2003).Mathematical model of indirect evaporative cooler using porous ceramic and heat pipe.*Applied Thermal Engineering 24*, 457-470.

Shao, L., Ibrahim, E., & Riffat, S. (2003). Ceramic Coolers for Building Passive Cooling.

Velasco Gomez, E., Rey Martinez, F., Varela Diez, F., Molina Leyva, M., & Herrero Martin, R. (2005). Description and experimental results of a semi-indirect ceramic evaporative cooler. *International Journal of Refrigeration* , 654-662.